IPTV with Rateless Channel Coding and Data-Partitioning for Broadband Wireless

Laith Al-Jobouri
University of Essex,
Colchester
United Kingdom
+44-1206-872817
lamoha@essex.ac.uk

Martin Fleury
University of Essex
Colchester
United Kingdom
+44-1206-872817
fleum@essex.ac.uk

Mohammed Ghanbari
University of Essex
Colchester
United Kingdom
+44-1206-872434
ghan@essex.ac.uk

ABSTRACT
Broadband wireless delivery of IPTV is under active investigation, though this environment is challenging. This paper examines the threat from slow and fast fading, traffic congestion, and channel packet drops. The proposed response is a combination of: rateless channel coding, which is adaptively applied; data-partitioned source coding to exploit prioritized packetization; and redundant slice provision, which is the focus of the evaluation in this paper. When fast and slow fading occur, this paper shows that redundant slices are certainly necessary but this provision is more effective for medium-quality video than it is for high-quality video.

Categories and Subject Descriptors
C.2.1 [**Computer-Communication Networks**]: Network Architecture and Design -*Wireless communication.*

General Terms
Algorithms, Performance, Experimentation.

Keywords
Data-partitioning, IEEE 802.16, IPTV, rateless channel coding, redundant slices.

1. INTRODUCTION
IPTV services include live TV program-on-demand, as well as time-shifted TV [1], both of which require unicast streaming. However, if this form of IPTV is to be extended to mobile devices then wireless access [2] presents a challenging environment for video streaming, especially if sport scenes are streamed, as these often contain rapid motion, leading to high temporal coding complexity. Burst errors can disrupt the fragile compressed bitstream (because of predictive coding dependencies), while error control should not increase end-to-end latency because of display and decode deadlines. However, as intelligent content management of IPTV moves popular material nearer to the end-user [3], it becomes feasible to combine application-layer channel coding with retransmission of additional redundant data without incurring prohibitive delays. The contribution of this paper is a combination of: rateless channel coding, which is adaptively applied; data-partitioned source coding to exploit prioritized packetization; and redundant slice provision, which is the focus of the evaluation in the paper.

In the time division duplex (TDD) form of multiplexing favored by broadband wireless access networks such as IEEE 802.16e (mobile WiMAX) [4], application-layer Automatic Repeat reQuests (ARQs) come almost for free by virtue of the return sub-frame. Therefore, a form of type 1 hybrid ARQ is possible. To achieve this, an adaptive form of rateless channel coding which utilizes such retransmissions is described in this paper. To avoid the long start-up delays that arise from packet erasure correction, error correction in the proposed scheme is at the byte level. Consequently, channel coding is powerless against packet drops, as obviously a packet is lost through buffer overflow before forward error correction (FEC) can be applied. In the same way, outright packet drops on the channel can occur, for example if the signal strength fails to reach a desired thresholding level. The most likely cause of this type of loss (assuming the mobile station remains in range) is a change in the wireless environment leading to slow fading. Therefore, further protection is required, which in this paper is provided by redundant video slices (a slice is a self-contained subset of a video frame's compressed data). Paradoxically, in the scenario investigated redundant slices with packets are more effective in their role in also duplicating the retransmission of corrupted packets than they are in protecting against outright packet drops.

We have also employed video data-partitioning [5] which is a form of error-resilient source coding in which the compressed video data are reorganized according to decoding priority. In an H.264/AVC (Advanced Video Coding) codec [6], data are partitioned between packets rather than re-ordered within a packet (refer to Section 2 for details). In particular, motion vectors (MVs) are packed into a partition-A slice packet, allowing error concealment to reconstruct missing partition-C slices containing texture data (quantized transform coefficient residuals). One advantage of this arrangement is that, as these packets are usually relatively smaller than the other packets, then these packets are less likely to be corrupted by channel noise.

However, in order to implement redundant slice protection it is not convenient in H.264/AVC to change the quantization parameter (QP) of redundant data-partitioned slices as normally occurs [7]. This is because, though both redundant slices and data-partitioned slices coexist in the Extended profile, they are not jointly implemented in the JM implementation of H.264/AVC [8] and, in fact, appear to not to be implemented at all in most other software implementations such as QuickTime, Nero, and LEAD randomly to name a few. However, it is possible with data-partitioning to create a duplicate stream of all partition-A slice packets or a duplicate stream consisting of partition-A and partition-B packets or, indeed, a replica of the original stream. Unequal error protection (UEP) is also associated with data partitioning such as using hierarchical modulation in [9]. However, the combined

congestion and channel error protection in the proposed scheme negates the need for UEP.

The feasibility of video streaming has recently been established [10] by means of a live WiMAX testbed. However, that study concentrated on varying the configuration parameters and used UDP-transported streams seemingly without congestion or error control. Other work in [11] is primarily concerned with combining true- and near-video-on-demand, providing a solution to how content should be allocated between the two services. Therefore, it further illustrates a scheme to bring content nearer the user. In [12], adaptive multicast streaming was proposed using H.264/SVC (Scalable Video Coding). Fixed WiMAX channel conditions were monitored in order to vary the bitrate accordingly. Unfortunately, the subsequent decision of the JVT standardization body for H.264/AVC *not* to support fine-grained scalability (FGS) implies that it will be harder to respond to channel volatility. Other work has also investigated combining scalable video, with multi-connections in [13] and in comparison with H.264/AVC in [14]. However, the data-dependencies between layers in H.264/SVC medium grained scalability are a concern, as, unlike in FGS, enhancement layer packets may successfully arrive but be unable to be reconstructed if key pictures fail to arrive. Instead, data-partitioning in our paper can be viewed as a simplified form of SNR layering [15] which can be protected against congestion drops through redundant slices. Temporal scalability is avoided because of its impact on media synchronization, especially lip synchronization.

There remains the problem of channel errors, which in this paper are guarded against in two ways. Firstly, to reduce temporal error propagation in H.264/AVC it is possible to place intra-refresh macroblocks (MBs) amongst the normally inter-coded MBs of P-pictures. These MBs appear with naturally encoded inter-coded MBs within partition-B slices. Because intra-coded MBs do not employ the predictive coding of P-pictures, they are not efficiently coded and, hence, they are not economical to use beyond about 5% per P-picture.

A more important form of protection is the use of application-layer FEC, which in this paper is through rateless channel coding [16]. Raptor coding [17] is a systematic variety of rateless code that does not share the high error floors [18] of prior rateless codes. It also has O(n) decode computational complexity. Rateless codes are a probabilistic channel code in the sense that reconstruction is not guaranteed. Because Raptor coding is indeed rateless, it is possible to adaptively vary the amount of redundant data according to an estimate of the channel conditions. It is also possible to piggyback additionally generated redundant data if the estimate is insufficient to allow reconstruction of the packet. However, further details are reserved for Section 3. The paper now establishes the video coding background before describing the adaptive scheme in Section 3.

2. DATA-PARTITIONING

The H.264/AVC codec conceptually separates the Video Coding Layer (VCL) from the Network Abstraction Layer (NAL). The VCL specifies the core compression features, while the NAL supports delivery over various types of network. In a communication channel the quality of service is affected by the two parameters of bandwidth and the probability of error. Therefore, as well as video compression efficiency, which is provided for through the VCL layer, adaptation to communication channels should be carefully considered. The concept of the NAL, together with the error resilience features in H.264, allows communication over a variety of different channels. Table 1 is a summarized list of different NAL unit types. NAL units 1 to 5 contain different VCL data that will be described later. NAL units 6 to 12 are non-VCL units containing additional information such as parameter sets and supplemental information.

In the H.264/AVC codec, each frame can be divided into several slices; each of which contains a flexible number of MBs. Variable Length Coding (VLC) that is entropy coding of the compressed data takes place as the final stage of the hybrid codec. In H.264/AVC, arithmetic coding replaced other forms of entropy coding in earlier codecs. In each slice, the arithmetic coder is aligned and its predictions are reset. Hence, every slice in the frame is independently decodable. Therefore, they can be considered as resynchronization points that prevent error propagation to the entire picture. Each slice is placed within a separate NAL unit (see Table 1). The slices of an Instantaneous Decoder Refresh- (IDR-)[1] or I-picture (i.e. a picture with all intra slices) are located in type 5 NAL units, while those belonging to a non-IDR or I-picture (P- or B-pictures) are placed in NAL units of type 1, and in types 2 to 4 when data partitioning mode is active, as now explained.

In type 1 and type 5 NALs, MB addresses, motion vectors (MVs) and the transform coefficients of the blocks, are packed into the packet, in the order they are generated by the encoder. In Type 5, all parts of the compressed bitstream are equally important, while in type 1, the MB addresses and MVs are much more important than the (integer) Discrete Cosine Transform (DCT) coefficients. In the event of errors in this type of packet, the fact that symbols appearing earlier in the bit-stream suffer less from errors than those which come later[2] means that bringing the more important parts of the video data (such as headers and MVs) ahead of the less important data or separating the more important data altogether for better protection against errors can significantly reduce channel errors. In the standard video codecs, this is known as data partitioning.

However, in H.264/AVC when data partitioning is enabled, every slice is divided into three separate partitions and each partition is located in either of type-2 to type-4 NAL units, as listed in Table 1. A NAL unit of type 2, also known as partition A, comprises the most important information of the compressed video bit stream of P- and B-pictures, including the MB addresses, MVs, and essential headers. If any MBs in these pictures are intra-coded, their DCT coefficients are packed into the type-3 NAL unit, also known as partition B. Type 4 NAL, also known as partition C, carries the DCT coefficients of the motion-compensated inter-picture coded MBs.

[1] An IDR picture is confusedly equivalent to an I-picture in previous standards. An I-picture in H.264/AVC allows predictive references beyond the boundary of a GOP.

[2] Because of the cumulative effect of VLC, symbols nearer the slice synchronization marker suffer less from errors than those that appear later in a bitstream.

Table 1. NAL unit types

NAL unit type	Class	Content of NAL unit
0	-	Unspecified
1	VCL	Coded slice
2	VCL	Coded slice partition A
3	VCL	Coded slice partition B
4	VCL	Coded slice partition C
5	VCL	Coded slice of an IDR picture
6-12	Non-VCL	Suppl. info., Parameter sets, etc.
13-23	-	Reserved
24-31	-	Unspecified

Fig. 1 is a comparison between the relative sizes of the partitions according to QP for the video clip which is employed in Section 5's evaluation. The test sequence was *Football*, which is a scene with rapid movement and consequently has high temporal coding complexity. This sequence is of a content type that quality of experience subjective testing indicates currently provides a difficult viewing experience [19] on mobile devices. *Football* was Variable Bit Rate (VBR) encoded at Common Intermediate Format (CIF) (352×288 pixel/picture), with a Group of Picture (GOP) structure of IPPP….. at 30 Hz, i.e. one initial intra-coded I-picture followed by all predictive P-pictures. This arrangement removes the complexity of bi-predictive B-pictures at a cost in increased bit rate. From the Figure it is apparent that the partition-B's contribution increases as the percentage of intra-refresh MBs grows, making partition-B packets more vulnerable to congestion and channel error as a result. The size of partition-C bearing packets declines with increasing QP as a result of coarser quantization of DCT coefficients. Notice that the range of QP in H.264/AVC is 0–51 with higher values corresponding to higher compression ratios and lower quality video.

In the context of H.264/AVC data-partitioning, it should be pointed out that though partition-A is independent of partitions B and C, *constrained intra prediction* should be set [15] to make partition-B independent of partition-C. However, partition-C cannot be made independent of partition-B if the Context-Adaptive Variable Length Coding (CAVLC) option is set. As data-partitioning is currently only enabled in the H.264/AVC Extended profile, whereas the alternative Context Adaptive Binary Arithmetic Coding (CABAC) option is not available in the Extended profile, it seems that partition-C is inevitably dependent on partition-B.

3. ADAPTIVE SCHEME

3.1 Packetization

To try to ensure corrupted packets are reconstructed if the original estimated redundant data is insufficient for reconstruction, the IPTV scheme works by retransmitting piggybacked redundant data. To reduce latency, the number of such retransmissions, after an ARQ over the uplink, was limited to one. A corrupt packet can be detected by the Cyclic Redundancy Check (CRC) that is an optional part of a MAC Protocol Data Unit (MPDU) (WiMAX packet), refer to Fig. 2. Though this CRC also applies to the 4-byte MAC header, it does indicate the likelihood that a packet's payload is corrupt. Then, through measurement of channel conditions, an estimate of the number of symbols successfully received is made. The WiMAX standard already specifies that a

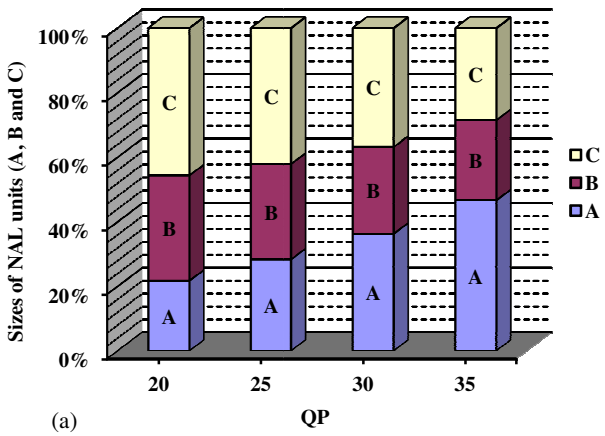

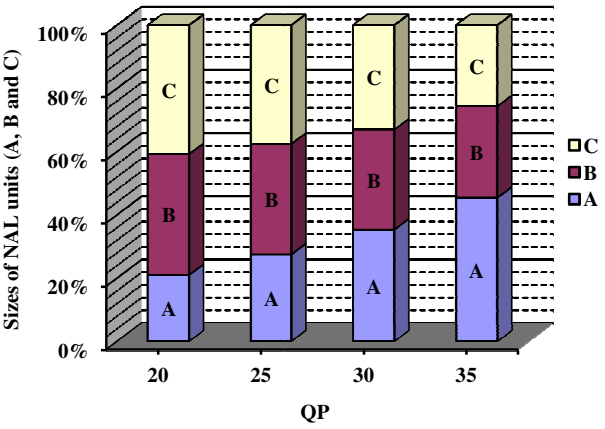

Figure 1. Relative sizes of data partitions according to quantization paramater (QP) for the *Football* video sequence, with (a) 5% intra-coded refresh MBs, and (b) 25% intra-coded refresh MBs.

station should provide channel measurements that can form a basis for channel quality estimates. These are either Received Signal Strength Indicators or may be Carrier-to-Noise-and-Interference Ratio measurements made over modulated carrier preambles.

Fig. 3 shows how ARQ triggered retransmissions works. In the Figure, the payload of packet X is corrupted to such an extent that it cannot be reconstructed. Therefore, in packet X+1 some extra redundant data (see Section 3.2) is included up to the level that its failure is no longer certain. If the extra redundant data is insufficient to reconstruct the original packet's payload, the packet is simply dropped. Otherwise, of course, it is passed to the H.264/AVC decoder.

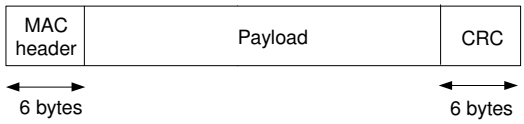

Figure 2. General format of a MAC PDU with optional CRC.

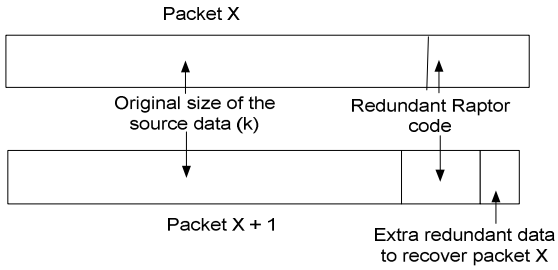

Figure 3. Division of payload data in a packet (MPDU) between source data, original redundant data and piggybacked data for a previous errored packet.

3.2 Rateless code modeling

In order to model Raptor coding, we employed the following statistical model [20]:

$$P_f(m,k) = 1 \quad \text{if } m < k,$$

$$= 0.85 \times 0.567^{\,m-k} \text{ if } m \geq k, \qquad (1)$$

where $P_f(m,k)$ is the failure probability of the code with k source symbols if m symbols have been received. Notice that the authors of [20] remark and show that for $k > 200$ the model almost perfectly models the performance of the code. In the experiments reported in this paper, the symbol size was set to bytes within a packet. Clearly, if instead 200 packets are accumulated before the rateless decoder can be applied (or at least equation (1) is relevant) there is a penalty in start-up delay for the video stream and a cost in providing sufficient buffering at the mobile stations.

To establish the behavior of rateless coding under WiMAX the well-known ns-2 simulator augmented with a module from the Chang Gung University, Taiwan [21] that has proved an effective way of modeling IEEE 802.16e's behavior.

We introduced a two-state Gilbert-Elliott channel model [22] in the physical layer of the simulation to simulate the channel model for WiMAX. To model the effect of slow fading at the packet-level, the *PGG* (probability of being in a good state) was set to 0.95, *PBB* (probability of being in a bad state) = 0.96, *PG* (probability of packet loss in a good state) = 0.02 and *PB* (probability of packet loss in a bad state) = 0.01 for the Gilbert-Elliott parameters. Additionally, it is still possible for a packet not to be dropped in the channel but, nonetheless to be corrupted through the effect of fast fading (or other sources of noise and interference). This byte-level corruption was modeled by a second Gilbert-Elliott model, with the same parameters (applied at the byte level) as that of the packet-level model except that *PB* (probability of byte loss) was increased to 0.165.

In the adaptive scheme, the probability of channel byte loss through fast fading (*BL*) in the Gilbert-Elliott model serves to predict the amount of redundant data to be added to the payload (*Redundant Raptor code* in Fig. 3). If *PGB* and *PBG* are the probabilities of going from good to bad state and from going from bad to good state respectively, then

$$\pi_G = PBG/(PBG + PGB) \qquad (2)$$

$$\pi_B = PGB/(PBG + PGB) \qquad (3)$$

are the steady state probabilities of being in the good and bad states. Consequently, the mean probability of channel corruption is given by

$$BL_{mean} = \text{PG}.\ \pi_G + \text{PB}.\ \pi_B \qquad (4)$$

that is the mean of a Uniform distribution in this case.

The instantaneous *BL* (taken from a Uniform distribution with mean BL_{mean}) is used to calculate the amount of redundant data adaptively added to the payload. If the original packet length is *L*, then the redundant data is given simply by

$$R = L\times BL+(L\times BL^2)+(L\times BL^3)\ldots \qquad (5)$$
$$= L/(1-BL),$$

which adds successively smaller additions of redundant data, based on taking the previous amount of redundant data multiplied by *BL*.

Assuming perfect channel knowledge of the channel conditions when the original packet was transmitted establishes an upper bound beyond which the performance of the adaptive scheme cannot improve. However, we have included measurement noise to test the robustness of the scheme. Measurement noise was modelled as a zero-mean Gaussian (normal) distribution and added up to a given percentage to the packet loss probability estimate.

If it turns out (by reference to the CRC in Fig. 2) that the packet cannot be reconstructed, despite the provision of redundant data then extra redundant data are added to the next packet (*Extra redundant data* in Fig. 3). Through measurement of channel conditions, an estimate of the number of symbols successfully received is made, giving a value *m'*. This implies from (1) that if less than *k* symbols (bytes) in the payload are successfully received then *k-m'+e* redundant bytes can be sent to reduce the risk of failure. In the evaluation tests, $e = 4$, resulting in a risk of less than 9% of packet loss, because of the exponential decay of the risk evident from equation (1).

3.3 Video configuration

The *Football* video sequence with the same configuration as for Fig. 1 was also selected for the WiMAX downlink tests. As a Group of Picture structure of IPPP.... was employed, it is necessary to protect against error propagation in the event of inter-coded P-picture slices being lost. To ensure higher quality video, 5% intra-coded MBs (randomly placed) were included in each frame (apart for the first I-picture) to act as anchor points in the event of slice loss. By employing a cyclic pattern of intra-refresh MBs [23], the reconstruction performance can be improved but this gives less flexibility in judging the impact of a given percentage of intra-coding support. The JM 14.2 version of the H.264/AVC codec software was employed, with the Evalvid framework [24] used to reconstruct sequences, according to reported packet loss from the simulator, and to assess the video quality (PSNR) relative to the input YUV raw video. Lost partition-C slice packets were compensated for by motion copy error concealment at the decoder using the MVs in partition-A. From Section 2, for high- to medium-quality video, the size of partition-A is relatively smaller in length than the other two partitions and, therefore, less likely to suffer from channel error. Similarly, partition-B is generally smaller than partition-C, provided that the intra-refresh MB contribution is kept to a low percentage (as herein).

4. WIMAX MODEL

The physical layer (PHY) settings selected for WiMAX simulation are given in Table 2. The antenna is modeled for comparison purposes as a half-wavelength dipole, producing an omni-directional emission pattern that is radiating power uniformly in one plane with a directive pattern shape in a perpendicular plane, i.e. as a slightly flattened torus. Omni-directional antennas are suitable for point-to-multipoint communication, possibly at a hotspot. Directional sector antennas can improve the signal and there are adaptive beam-forming systems as well. Panel antennas can be used for point-to-point transmission and WiMAX has been augmented with MIMO antenna. However, modeling a different antenna would distort the generality of the findings. The antenna heights are standard ones recommended by the WiMAX forum as are the transmit powers. These settings result in a range of about 1 km if Orthogonal Frequency Division Multiple Access (OFDMA) is used. OFDMA allows partitioning of the OFDM sub-channels between multiple users.

The TDD frame length was set to 5 ms, as this is the value that seems to be commonly implemented, probably because it is the only length specified by the WiMAX forum. It is possible that longer durations, up to 20 ms in the IEEE Standard [4] may be more advantageous for video streaming as this duration allows more packets to be removed from Subscriber Station (SS) queues at any one polling instance.

There is a mandatory channel coding scheme for mobile WiMAX which is applied on a block-by-block basis. The coder is a binary non-recursive convolutional coder with a constraint length of seven resulting in a native code rate of 1/2. Other more powerful channel coders such as convolutional turbo codes are specified as optional. It is worth noting that, though these channel coding systems are available in 3GPP systems, application-layer channel coding was still found to be necessary [25] in the Multimedia Broadcast-Multicast Service. Hybrid ARQ (HARQ) at the physical layer is an optional feature, which in the simulation model is assumed to be turned off. The effect of HARQ could be to introduce uncontrollable latencies from repeated ARQs, which would impact the streaming performance. Introducing a guard band interval of 1/8 allows a maximum datarate of 10.67 Mbps with 16-QAM (Quadrature Amplitude Modulation), provided that the downlink/uplink sub-frame ratio is 3:1. This is appropriate, as a Base Station (BS) requires greater access to the channel as it must service multiple SSs. The 16-QAM ½ coding rate with 1/8 guard band is one of the mandatory coding modes for WiMAX.

Video was transmitted from a BS over the downlink with UDP-lite [26] transport. The advantage of UDP-lite is that it can be configured to pass corrupted as well as uncorrupted packets to the application layer, restricting the UDP CRC to the UDP header. In order to introduce sources of traffic congestion, an always available FTP source was introduced with TCP transport to a second SS. Likewise a CBR source with packet size of 1000 B and inter-packet gap of 0.03 s was also downloaded to a third SS. While the CBR and FTP traffic occupies the non-rtPS (non-real-time polling service) queue, rather than the rtPS queue, they still contribute to packet drops in the rtPS queue for the video, if the packet rtPS buffer is already full or nearly full, while the nrtPS queue is being serviced. Sender buffer sizes were set to fifty packets[3]. We are aware that this congestion configuration is just one of many and future work should investigate this dimension of the problem.

Table 2. IEEE 802.16e parameter settings.

Parameter	*Value*
PHY	OFDMA
Frequency band	5 GHz
Bandwidth capacity	10 MHz
Duplexing mode	TDD
Frame length	5 ms
Max. packet length	1024 B
Raw data rate	10.67 Mbps
IFFT size	1024
Modulation	16-QAM 1/2
Guard band ratio	1/8
MS transmit power	245 mW
BS transmit power	20 W
Approx. range to SS	1 km
Antenna type	Omni-directional
Antenna gains	0 dBD
MS antenna height	1.2 m
BS antenna height	30 m

OFDMA = Orthogonal Frequency Division Multiple Access, QAM = Quadrature Amplitude Modulation, TDD = Time Division Duplex

5. EVALUATION

Three types of erroneous packets were considered: 1) packet drops at the BS sender buffer 2) packet drops through channel noise and interference, especially slow fading and 3) corrupted packets that were received but affected by Gilbert-Elliott channel noise to the extent that they could not be immediately reconstructed without an ARQ triggered retransmission of piggybacked redundant data. Notice that if the retransmission of additional redundant data still fails to allow the original packet to be reconstructed then the packet is simply dropped. The Raptor code equation (1) was applied to decide if a packet could be recovered, given the number of bytes that were declared to be in error.

In Table 3, three schemes are compared, all of which adaptively include redundant data according to the description of Section 3.2. In the mean, 5% additive Gaussian measurement noise was applied to the estimate of *BL* in (5) to make the adaptive schemes more realistic. The scheme labeled *1 slice NAL* treats a picture as a single slice but creates the three data partitions (A, B, and C) described in Section 2. The scheme labeled *2 slice NAL* geometrically divides each picture into two horizontal slices. Each of the two slices is split into three data partitions and as before each forms a NAL unit. Each NAL unit occupies an IP/UDP/RTP packet, which, after packetization as a MAC Service Data Unit, occupies a single WiMAX MAC PDU. The main effect of the two slice scheme is to reduce packet sizes. The scheme labeled *Redundant NAL* also includes the redundant slice packets, which in Table 3 means redundant partition-A, -B, and -C packets (all packets replicated). The *Redundant NAL* scheme is a single slice

[3] In WiMAX terms, a packet herein consists of a Media Access Control (MAC) Service Data Unit (MSDU) passed to the data link layer encapsulated in a MAC Protocol Data Unit (MPDU) at the PHY layer.

per picture scheme and, hence, no advantage is gained from smaller packet sizes. 5% intra-refresh data were added to each picture, increasing the size of partition-B packets (refer to Fig. 1).

In Table 3, the Redundant NAL scheme extends to all partitions. This does *not* amount to a change in bitrate because the packets are simply replicated. However, the end-to-end packet delay will obviously increase because of the interleaving of the redundant slice packets. Notice also that the number of packets sent for the two slice scheme is the same as for the redundant slice packet scheme.

Though only a moderate percentage of one slice scheme packets (6.9%) are dropped outright from the combined effects of congestion and channel conditions, this results at QP = 20 to a PSNR of only 19.98 dB, that is, it is at an unnacceptable level. Unfortunately, though the percentage of packets dropped reduces (because of the smaller packet sizes), the sending quality is reduced at higher QPs, with the result that the objective quality at the receiver display remains below 25 dB, that is approxiamtely equivalent to a poor rating in the ITU P.800's [27] subjective mean opinion score scale. Packet size has a significant effect, as in the two-slice scheme video quality is increased. However, reducing the packet size is still insufficient (video quality below 25 dB) when faced with the combined effect of packet drops and channel conditions.

In the redundant NAL scheme, retransmission of extra redundant data was scheduled for all corrupted packets, even if two packets duplicated each other. This is because it is not possible to know in advance whether the extra redundant data will arrive for any one of the two packets. This provision has a significant effect in improving the video quality at higher QPs. The reason is that retransmitting extra redundant data by two alternative means increases the chance that a packet can be reconstructed. Overall video quality is approximately equivalent (above 31 dB) to the ITU P.800 'good' category at the higher QPs illustrated.

At lower QPs for the redundant NAL scheme, higher packet drop rates occur (23.1 % and 4.1%). The packet size at QP = 20 is large and the effect of sending such packets in duplication contributes to the high loss rate. Therefore, at low QP it appears that redundant slice provision is *not* an effective guard against packet drops Unfortunately also, for lower QPs total end-to-end delay for both corrupted and normal packets is high and there is a possibility of interruptions. The throughput of the WiMAX channel is likely to remove the risk of display interruptions at higher QP delay times.

Table 4 is an analysis of packet drops from channel loss alone, i.e. by application of the Gilbert-Elliot packet loss model of Section 3.2. From this analysis it is apparent that at lower QPs, packet drop numbers are distributed in inverse order of data priority. This should not be surprising as higher priority packets (partition-A and -B packets) are smaller at lower QPs and, hence, in the mean spend less time exposed to the channel. A surprising feature of this Table is that in the redundant NAL scheme at higher QPs, few if any packets are dropped when traversing the channel (or from Table 3 are dropped at the BS send buffer). Because the packet sizes are small at these QPs, packet drops are generally less than 2% (except for QP = 30 in the one slice NAL scheme). However, the reason for the few drops is under further investigation.

Naturally it was of interest to us whether it was possible to employ only redundant partition-A slice packets or only redundant partition-A and partitition-B slices packets. These two options are examined in Table 5. Table 6 performs an equivalent analysis to

Table 3. Mean performance metrics when streaming *Football*, when redundant NAL protection extends to all partitions.

	Dropped packets (%)		
QP	1 slice NAL	2 slice NAL	Redundant NAL
20	6.9	1.9	23.1
25	4.2	2.8	4.9
30	4.0	1.9	0.1
35	1.7	1.2	0.0
	Corrupted packets (%)		
QP	1 slice NAL	2 slice NAL	Redundant NAL
20	30.8	22.2	14.5
25	30.6	24.4	25.1
30	27.6	22.2	27.0
35	21.9	17.1	22.4
	PSNR (dB)		
QP	1 slice NAL	2 slice NAL	Redundant NAL
20	19.98	23.38	18.04
25	20.96	22.84	21.72
30	21.16	21.74	35.27
35	23.27	25.22	33.45
	Corrupted packet mean delay (s)		
QP	1 slice NAL	2 slice NAL	Redundant NAL
20	0.023	0.012	0.133
25	0.020	0.013	0.083
30	0.018	0.012	0.019
35	0.017	0.011	0.017
	Packet end-to-end delay (s)		
QP	1 slice NAL	2 slice NAL	Redundant NAL
20	0.012	0.007	0.112
25	0.010	0.008	0.071
30	0.008	0.007	0.009
35	0.007	0.006	0.007

Table 4 and equally shows that higher priority data packets benefit from size-dependent packet losses on the channel. However, though other performance metrics are favorable, and though protection of both partition-A and partition-B slice packets is preferable, results show that in this scenario and for the *Football* video sequence protection of partition-C is necessary to reconstruct the stream to a satisfactory quality. We attribute this to the high motion present in the *Football* reference sequence as this implies that succeeding frames may be very different. As a result, error concealment by motion vectors alone may be insufficient.

6. CONCLUSION

Though a form of hybrid ARQ has been applied in this paper and though an advanced form of packetization (data-partitioning) was combined with adaptive rateless coding, it is still very possible that unacceptable video quality can occur when streaming over a

broadband wireless channel. This is particularly so if there is high motion in the streamed video, which unfortunately includes many sports scenes. Redundant slices were provided originally as a counter to possible outright packet drops but paradoxically they proved of most worth in ensuring additional redundant data successfully arrived. Another observation is that careful choice of quantization parameter for VBR video is necessary, as too low a choice will result in large packets that are prone to loss or corruption in one of several ways. In future investigations, the adaptive scheme presented can be turned around in that instead of repairing lower priority data packets, these packets can be discarded if conditions do not merit transmission.

Table 4. Analysis of dropped packets from channel conditions in Table 3 according to partition type.

	No. of dropped packets		
	1 slice NAL		
QP	Partition-A	Partition-B	Partition-C
20	10	19	25
25	7	15	11
30	5	14	12
35	8	2	4
	2 slice NAL		
QP	Partition-A	Partition-B	Partition-C
20	6	13	11
25	10	16	18
30	6	13	11
35	8	5	5
	Redundant NAL		
QP	Partition-A	Partition-B	Partition-C
20	57	121	183
25	7	22	47
30	1	0	1
35	0	0	0

Table 5. Mean performance metrics when streaming *Football*, when various redundant NAL protections schemes are used.

	Dropped packets (%)	
QP	Redundant A	Redundant A, B
20	2.7	13.5
25	4.2	1.4
30	1.4	0.5
35	1.4	0.4
	Corrupted packets (%)	
QP	Redundant A	Redundant A, B
20	31.9	22.7
25	30.8	30.3
30	30.8	27.4
35	16.6	24.7
	PSNR (dB)	
QP	Redundant A	Redundant A, B
20	21.87	24.72
25	19.93	22.72
30	20.78	25.82
35	23.34	31.76
	Corrupted packet mean delay (s)	
QP	Redundant A	Redundant A, B
20	0.042	0.095
25	0.019	0.030
30	0.018	0.018
35	0.021	0.016
	Packet end-to-end delay (s)	
QP	Redundant A	Redundant A, B
20	0.032	0.083
25	0.009	0.019
30	0.008	0.008
35	0.007	0.007

7. REFERENCES

[1] Degrande, N., Laevens, K., and De Vleeschauwer, D. 2008. Increasing the user perceived quality for IPTV services. *IEEE Communs. Mag.*, 46, 2, 94-100.

[2] Wu, M., Makharia, S., Liu, H., Li., D., and Mathur, S. 2009. IPTV multicast over wireless LAN using merged hybrid ARQ with staggered adaptive FEC. *IEEE Trans. Broadcasting*, 55, 2, 363-374.

[3] De Vleeschauwer, D., and Laevens, K. 2009. Performance of caching systems for IPTV on-demand services. *IEEE Trans. Broadcasting*, 55, 2, 491-501.

[4] IEEE, 802.16e-2005. 2005. *IEEE Standard for Local and Metropolitan Area Networks. Part 16: Air Interface for Fixed and mobile Broadband Wireless Access Systems.*

[5] Li, A.H., Kittitornkun, S., Hu, Y.H., Park, D.S., and Villasenor, J.D. 2002. Data partitioning and reversible variable length codes for robust video communications. *Proc. of Data Compression Conf.*, 460-489.

[6] Wenger, S. 2003. H.264/AVC over IP. *IEEE Trans. Circuits Syst. Video Technol.*, 13, 7, 645-655.

[7] Radulovic, I., Wang, Y.-K., Wenger, S., Hallapuro, A., Hannuksela, M.H., and Frossard, P. 2007. Multiple description H.264 video coding with redundant pictures. *Proc. of Int'l Workshop on Mobile Video*, 37-42.

[8] Tourapis, A.M., Sühring, K., and Sullivan, G. 2009. H.264/14496-10 AVC Reference Software Manual. *31st Meeting of the Joint Video Team*, London, UK.

[9] Barmada, B., Mahdi, M. M., Jones, E.V., and Ghanbari, M. 2005. Prioritiised transmission of data-partitioned H.264 video with hierarchical QAM. *IEEE Sig. Proc. Letter*, 12, 8, 577-580.

[10] Issa, O., Li, W., and Liu, H. 2010. Performance evaluation of TV over broadband wireless access networks. *IEEE Trans. Broadcasting*, 56, 2, 201-210.

[11] Lee, L. M., Park, H.-J., Choi, S. G., and Choi, J. K. 2009. Adaptive hybrid transmission mechanism for on-demand mobile IPTV over WiMAX. *IEEE Trans. Broadcasting*, 55, 2, 468-477.

Table 6. Analysis of dropped packets from channel conditions in Table 5 according to partition type.

	No. of dropped packets		
	Redundant A		
QP	Partition-A	Partition-B	Partition-C
20	0	8	20
25	0	7	19
30	0	5	10
35	0	6	9
	Redundant A, B		
QP	Partition-A	Partition-B	Partition-C
20	26	80	70
25	2	0	16
30	0	0	6
35	1	0	4

[12] Hillested, O., Perkis, Genc, V., Murphy, S., and Murphy, J. 2007. Adaptive H.264/MPEG-4 SVC video over IEEE 802.16 broadband wireless access networks. *Proc. of Packet Video Workshop*.

[13] Juan, H.-H., Huang, H.-C. , Huang, C.Y., and Chiang, T. 2008. Cross-layer mobile wireless MAC designs for the H.264/AVC scalable video coding. *Wireless Networks*, 16, 1, 113-123.

[14] Casampere, J., Sanshez, P., Villameriel, T., and Del Ser, J. 2009. Performance evaluation of H.264/MPEG-4 Scalable Video Coding over IEEE 802.16e networks. *Proc. of IEEE Int'l Symp. on Broadband Multimedia Systems and Broadcasting*, 6 pages.

[15] Mys, S., Lambert, P., and De Neve, W. 2006. SNR scalability in H.264/AVC using data partitioning. *Proc. of Pacific Rim Conf. in Multimedia*, 329-338.

[16] MacKay, D.J.C. Fountain codes. 2005. *IEE Proc.: Communications*, 152, 6, 1062–1068.

[17] Shokorallahi, A. 2006. Raptor codes. *IEEE Trans. Information Theory*, 52, 6, 2551-2567.

[18] Palanki, R. and Yedidai, J. 2004. Rateless codes on noisy channels. *Proc. of Int'l Symp. Inform. Theory*.

[19] Agboma, F., and Liotta, A. 2007. Addressing user expectations in mobile content delivery. *Mobile Information Systems*, 3, 3/4, 153–164.

[20] Luby, M., Gasiba, T., Stockhammer, T., and Watson, M. 2007. Reliable multimedia download delivery in cellular broadcast networks. *IEEE Trans. Broadcasting,* 53, 1, 235-246.

[21] Tsai, F. C. D. et al. 2006. The design and implementation of WiMAX module for ns-2 simulator. *Workshop on ns2*, article no. 5.

[22] Haßlinger, G., and Hohlfeld, O. 2008. The Gilbert-Elliott model for packet loss in real time services on the Internet. *Proc. of 14th GI/ITG Conf. on Measurement, Modelling, and Evaluation of Computer and Commun. Systs.,* 269-283.

[23] Schreier, R. M., and Rothermel, A. 2006. Motion adaptive intra refresh for the H.264 video coding standard. *IEEE Trans. Consumer Electronics*, 52, 1, 249-253.

[24] Klaue, J., Rathke, B., and Wolisz, A. 2003. EvalVid - A framework for video transmission and quality evaluation. *Proc.* of *Int'l Conf. on Modeling Techniques and Tools for Computer Performance*, 255-272.

[25] Afzal, J., Stockhammer, T., Gasiba, T. and Xu, W. 2006. Video streaming over MBMS: A system design approach. *J. of Multimedia*, 1, 5, 25-35.

[26] Larzon, L.-A., Degermark, M., Pink, S., Jonsson, L.-E., and Fairhurst, G. 2004. The lightweight user datagram protocol (UDP-Lite). *IETF*, RFC 3828 (Jul. 2004).

[27] ITU-T Rec. P.800. 1996. Methods for subjective determination of transmission quality.